Contrib Mineral Petrol (2001) 141: 367–379
DOI 10.1007/s004100100254

Hong-Fu Zhang · Martin A. Menzies · Dave P. Mattey
Richard W. Hinton · John J. Gurney

# Petrology, mineralogy and geochemistry of oxide minerals in polymict xenoliths from the Bultfontein kimberlites, South Africa: implication for low bulk-rock oxygen isotopic ratios

Received: 22 May 2000 / Accepted: 20 January 2001 / Published online: 11 April 2001


**Abstract** Polymict mantle xenoliths from the Bultfontein kimberlites, South Africa, contain abundant ilmenites (30% in BD2666, 15% in JJG1414, 3% each in BD2394 and BD344). These ilmenites occur as disrupted veins or layers, coarse discrete grains, small segregations interstitial to other silicate minerals, and tiny irregular grains disseminated in the subgrains of enstatites. The vein-like ilmenite usually shows a textural zonation across the vein, in rare cases along veins. This textural zonation is coincident with chemical and oxygen isotopic variations, with the margins being finer in grain sizes and richer in incompatible elements. The chemical and isotopic compositions also vary between different occurrences of ilmenite grains. In general, the smaller grains are richer in Cr, LREE and LILE and lighter in oxygen isotopes. Thus, chemical and oxygen isotopic disequilibria are well preserved in these ilmenites, which are also seen in the silicate minerals. These features suggest that ilmenites from the polymict xenoliths formed by magmatic and/or metasomatic processes. The invasion of the Fe-Ti-Cr-rich melt with low oxygen isotopic ratio can account for the observed low bulk oxygen isotopic ratios in the polymict xenoliths. This Fe-Ti-rich melt with high ilmenite normative could be produced by melt immiscibility during the migration of an initially homogeneous high-Ti silicate melt.

**Keywords** South Africa · Polymict xenolith · Oxide mineral · Ilmenite · Chemical zoning

H.-F. Zhang (✉)
Laboratory of Lithosphere Tectonic Evolution,
Institute of Geology and Geophysics,
Chinese Academy of Sciences, P.O. Box 9825,
Beijing 100029, P.R. China
E-mail: hfzhang@mail.igcas.ac.cn
Tel.: +86-10-62007821
Fax: +86-10-62010846

H.-F. Zhang · M.A. Menzies · D.P. Mattey
Department of Geology,
Royal Holloway University of London,
Egham, Surrey TW20 OEX, UK

R.W. Hinton
Department of Geology and Geophysics,
The University of Edinburgh, West Mains Road,
Edinburgh EH9 3JW, UK

J.J. Gurney
Department of Geochemistry, University of Cape Town,
Rondebosch 7700, South Africa

Editorial responsibility: T.L. Grove

## Introduction

Oxide minerals are accessory constituents in kimberlites and kimberlite-borne mantle xenoliths. They are important because of their widespread occurrences in xenoliths from subcontinental lithospheric mantle, and the fact that they can provide diagnostic information about the composition of the melt migrated through the lithosphere. Examples are armalcolite and exotic oxides, such as lindsleyite-mathiasite (LIMA) and yimengite-hawthorneite (YIHA; e.g. Erlank et al. 1987; Haggerty 1991, 1994). Several authors have published analyses of oxide minerals (e.g. spinel, ilmenite and rutile) overgrown with silicate minerals in kimberlite megacrysts or in individual nodules (Wyatt 1979; Rawlinson and Dawson 1979; Gurney et al. 1979; Haggerty et al. 1979; Meyer et al. 1979; Pasteris et al. 1979). Erlank et al. (1987) outlined the occurrence of oxide minerals in garnet peridotites (GP), garnet phlogopite peridotites (GPP), phlogopite peridotites (PP), and phlogopite K-richterite peridotites (PKP) from Kimberley, South Africa. These authors noted that garnet lherzolites typically contain only minor amounts of sulphides, spinel, ilmenite, and rutile whereas garnet harzburgites are typified by chromian spinel with the absence of sulphides, ilmenite and rutile. In GPP and PP rocks, spinel coexists with garnet, enstatite and diopside. The texture may be vermiform or symplectitic. Small platelets and single spinel grains are also present. In the PKP rocks, the crichtonite mineral series, sulphides, armalcolites

(Arm), and even exotic oxides (LIMA and YIHA) may be found in association with K-richterite and rutile. Thus, it appears to be clear from those studies that spinel series minerals are the dominant Fe-Ti-rich oxides in kimberlite-borne mantle xenoliths. When ilmenite is present, it is normally associated with spinel or occurs as overgrowths surrounding silicate minerals, especially pyroxene. This is totally different from the observation in the polymict xenoliths in which ilmenite is present in association with rutile but not spinel (Wyatt and Lawless 1984; Zhang 1998). When ilmenite and rutile are present as major constituents in mantle xenoliths, they are dominantly associated with the mica-amphibole-rutile-ilmenite-diopside (i.e. MARID; Dawson and Smith 1977; Waters 1987), with ilmenite-rutile-phlogopite-sulphide (i.e. IRPS; Harte et al. 1987), or with other unusual xenoliths (e.g. Meyer et al. 1979). The occurrence of abundant ilmenite in the polymict xenoliths probably represents another unusual paragenesis. In this contribution, we will examine the petrographic, geochemical and oxygen isotopic characteristics of oxide minerals, in particular ilmenite, in these polymict xenoliths and discuss their formation.

## Petrology

The four polymict mantle xenoliths studied here are all from the Bultfontein kimberlites, South Africa. They contain nonequilibrium mineral assemblages derived from the Archaean South African lithospheric fragments of varied peridotitic provenance (Zhang 1998), and can be texturally classified as disrupted or mosaic porphyroclastic (Lawless et al. 1979). Detailed descriptions of the polymict xenoliths are given in Lawless et al. (1979) and Zhang (1998). Polymict peridotite JJG1414 contains about 15 volume% ilmenites as giant discrete grains (> 1 cm) or in disrupted "veinlets"/"layers" (Fig. 1a). A few ilmenite veins extend to 5 cm long. These ilmenites display a well-equilibrated, polygranular mosaic texture, and the subgrain boundaries are regular and slightly curved. Triple 120° junctions are common (Fig. 1b). Some vein-like ilmenite shows textural zonation (Fig. 1c) where the margins of the veins are finer in grain sizes than the cores. Tiny disseminated ilmenites and rutiles (Fig. 1d) are present in association with the replacement of diopside by enstatite. The sulphide phases are also found as intergrowths with discrete ilmenite. Polymict peridotite BD2666 contains about 30% ilmenites as irregular and disrupted layers or veins (Fig. 2a) nearly parallel to each other, and rock foliation. The sulphides also occur in a minor amount situated at the edge of ilmenite veins. These ilmenite layers or veins show distinctive deformation features characterised by the band or zone of polycrystalline ilmenite which is preferably oriented parallel to the vein and varies tremendously in subgrain sizes. Textural zonation has also been observed along a vein (Fig. 2b). In addition, some neoblastic olivine contains randomly distributed ilmenite needles (Fig. 2c). Oxide minerals in polymict peridotites BD2394

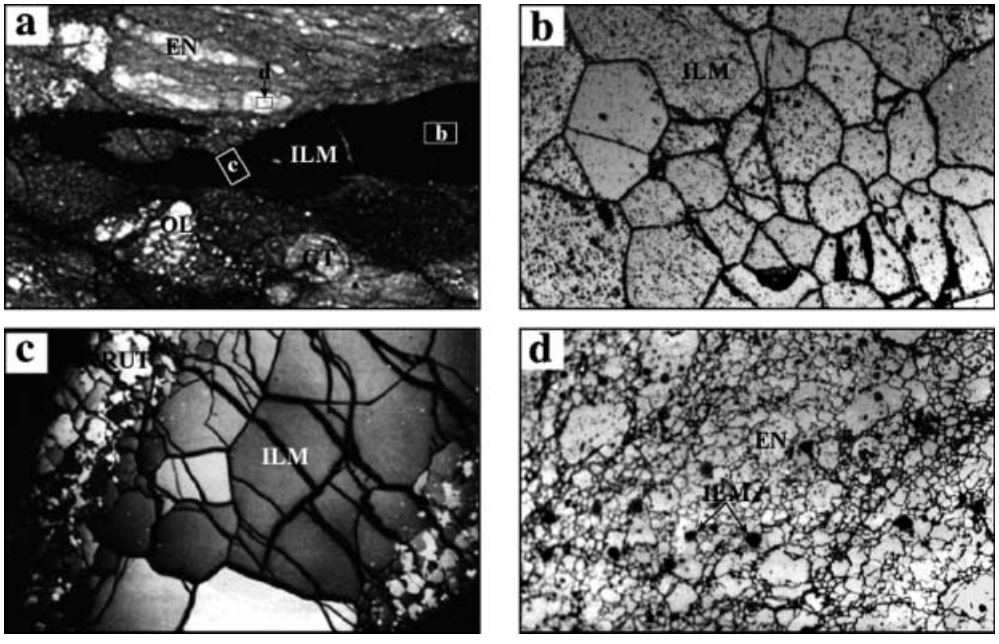


**Fig. 1a–d** Photographs of double-polished slices of a mosaic porphyroclastic polymict peridotite (JJG1414) in reflected light. **a** Disrupted ilmenite vein, together with porphyroclastic olivine, enstatite, and garnet, set in a fine-grained mylonitic olivine matrix (width of field = 30 mm). Characters *b, c, d in rectangles* Positions of Fig. 1b, c, and d respectively. **b** Well-defined triple junction ilmenite grains in the core of the vein indicate a textural equilibrium during the deformation process (width of field = 2 mm). **c** Textural zonation of an ilmenite vein (Wyatt and Lawless 1984), showing the fine-grained ilmenite and rutile concentrated on the edge relative to the coarse ilmenite grain in the core (width of field = 2 mm). **d** Fine-grained, disseminated ilmenites and mosaic subgrains of enstatite formed by mylonitisation (width of field = 1 mm). *OL* Olivine, *EN* enstatite, *GT* garnet, *ILM* ilmenite, *RUT* rutile

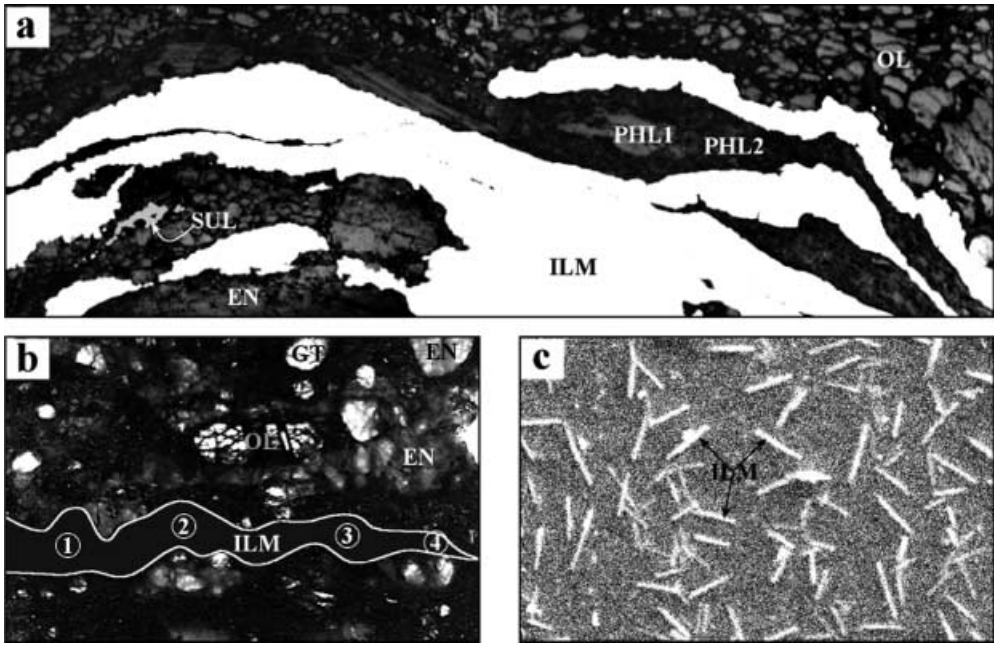


**Fig. 2** **a** Photomicrographs of double-polished slice of a laminated porphyroclastic polymict peridotite (BD2666) in reflected light. Irregular and disrupted ilmenite veins or layers and a few porphyroclastic enstatites set in fine-grained olivine and phlogopite matrices. Two forms of secondary phlogopite (i.e. large irregular phlogopite and tiny euhedral phlogopite aggregates) usually located at the margin of ilmenite vein or between veins. Sulphide minerals also occur in trace amounts (width of field = 4 mm). **b** Photographs of a double-polished rock slice (BD2666) in reflected light, showing porphyroclastic minerals (*OL*, *EN*, and *GT*) with the emphasis on a single ilmenite veinlet outlined by *open line*. This vein shows a systematic variation of elemental geochemistry from the wider section ① to the narrow terminal ④ (width of field = 24 mm). **c** Back-scattered image showing randomly distributed ilmenite needles in a neoblastic olivine (width of field = 0.2 mm). *OL* Olivine, *EN* enstatite, *GT* garnet, *ILM* ilmenite, *SUL* sulphide, *PHL1* large irregular phlogopite, *PHL2* tiny euhedral phlogopite aggregates

and BD344 are less abundant (~3%), and are mainly ilmenites with sparse rutile and sulphides. Unlike those in the above-mentioned polymict xenoliths, ilmenites in BD2394 and BD344 do not show textural zonation. Coarse ilmenites (>1 cm; Fig. 3a), small ilmenites (~0.2–1 mm; Fig. 3b, c), and tiny anhedral ilmenites (≤ 0.2 mm; Fig. 3d) disseminated in subgrained enstatite are all present in single polymict xenolith and are apparently not the products of the same stage. A few small or elongated rutiles, with ilmenite lamellae in one grain, are associated with ilmenites and secondary phlogopite. A few tiny sulphides are disseminated in brown subgrained enstatites or throughout the rocks.

## Methods

Major-element compositions for oxide minerals were analysed in situ on double-polished, carbon-coated slices using a JEOL Superprobe equipped with an energy disperse system (EDS) and an automation system (AN 10000/55S with 2,500 CPS) at the Geology Department of Birkbeck College, University of London. Analysis was performed with a focused beam of 15 KeV and 15 nA. The beam is focused onto a spot of ~1 μm diameter. ZAF4 are used for the online correction. Analytical uncertainties for major elements were estimated at the level of less than 1%, with most values varying between 0.2 and 0.5%. Trace-element abundances in ilmenites were measured on the same but gold-coated slices with a Cameca ims-4f ion microprobe at the Department of Geology and Geophysics, Edinburgh University. The measurements were made with an 8-nA $^{16}O^-$ primary beam accelerated by 10 KeV and focused to a spot 15–20 μm in diameter. Due to the lack of an ilmenite standard during the analysis, the trace-element abundance in ilmenite was expressed as counts per second (CPS). Generally, the more counts recorded, the higher the elemental concentrations in ilmenite. The precision of the recorded count for most trace elements is within 10%. Oxygen isotopic ratios in ilmenite were analysed on VG Prism using the laser-fluorination technique (Mattey and Macpherson 1993) at the Department of Geology, Royal Holloway University of London. The detailed sample preparation and analytical procedures are given in Zhang et al. (2000). Ten ilmenite samples (ca. 2 mg) and four San Carlos olivine standards were loaded within each batch run. San Carlos olivine standards gave a mean isotopic composition of $4.86 \pm 0.18‰$ ($n = 245$; Mattey et al. 1994b). Equipment consistency was also checked for the reproducibility of duplicate runs, and the discrepancy between runs was commonly less than 0.2‰.

## Results

### Major elements

#### *Ilmenite*

Ilmenite compositions in the Bultfontein polymict peridotites, South Africa, are presented in Tables 1 and 2. It is obvious from Tables 1 and 2, and Fig. 4a–b that ilmenites in these peridotites are rich in MgO (>12 wt%) and can be termed as pricroilmenites. Pricroilmenites are also characterised by high $Cr_2O_3$ and $TiO_2$ but relatively low FeO contents (<30 wt%). Large portions of ilmenites contain $Nb_2O_5$, with a tiny one in BD2394

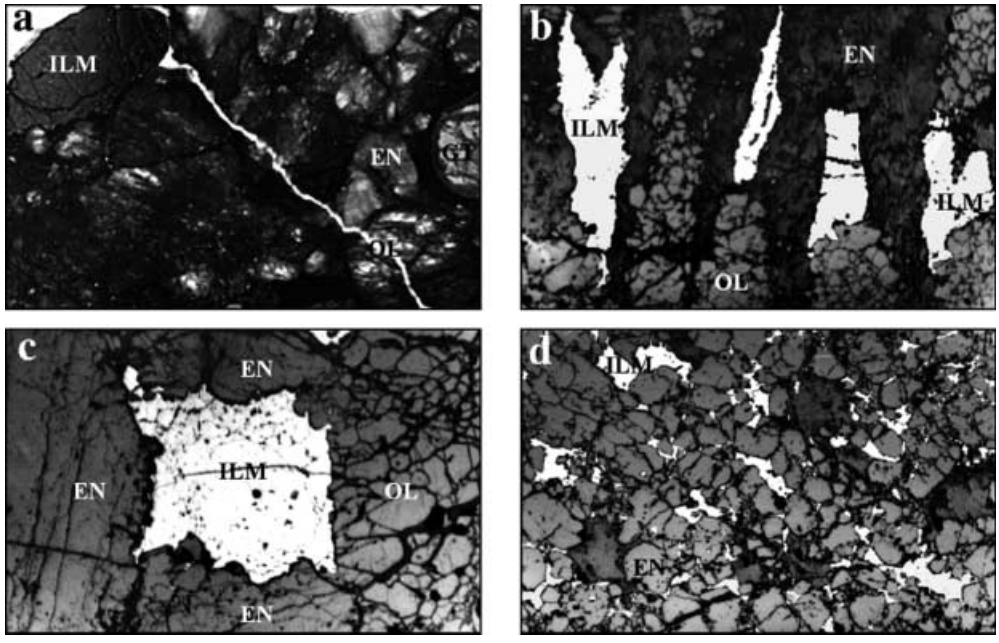


**Fig. 3a–d** Photomicrographs of double-polished slices of the polymict peridotites (BD2394 and BD344) in reflected light, illustrating different occurrences of ilmenites. **a** Coarse ilmenite and *OL*, *EN*, and *GT* in BD344 (width of field = 17 mm). **b** and **c** Small and/or elongated ilmenites segregated between OL and EN in BD2394 (width of field = 2 mm). **d** Tiny anhedral ilmenites and a few sulphide grains disseminated in brown subgrains of sheared enstatite in BD2394 (width of field = 2 mm). *OL* Olivine, *EN* enstatite, *GT* garnet, *ILM* ilmenite

containing up to 0.8 wt%. Overall, ilmenites in the polymict xenoliths have relatively constant compositions, and all plot within the field for transitional ilmenites in association with YIHA (Fig. 4a; Haggerty 1991, 1994). They are compositionally distinct from the kimberlite-borne megacrystic ilmenites, which are lower in MgO.

Ilmenite compositions also vary in the polymict rocks, even in individual grains (Fig. 4b–c). Ilmenites from JJG1414 have relatively constant $Cr_2O_3$ and low FeO contents, except the rims (Table 1). However, their MgO (Fig. 4b), $Al_2O_3$ (Fig. 4c) and $TiO_2$ contents (56.4–57.4 wt%) are slightly higher than those in the other three phlogopite-bearing peridotites. Additionally, as noted above, ilmenite occasionally shows a textural zonation, which is a reflection of compositional variations, particularly for $Cr_2O_3$. The polycrystalline ilmenite rim shows much higher $Cr_2O_3$ levels than the well-equilibrated core (Fig. 4b–c). However, MgO contents are essentially constant from rim to core (Fig. 4b). $Cr_2O_3$ can be as high as 5 wt% (Wyatt and Lawless 1984), and abruptly drops to $< 2.5$ wt% within 1.4 mm. Ilmenite from BD2666 exhibits a constant MgO content ($12.6 \pm 0.2$ wt%) and a low $Nb_2O_5$ content (0.1–0.2 wt%). The range of $Cr_2O_3$ and $Al_2O_3$ is also restricted (Fig. 4c). It should be noted that ilmenite compositions vary from vein to vein and within veins. Along one veinlet (Fig. 2b), the $Cr_2O_3$ and $Al_2O_3$ contents increase (Table 2 and Fig. 4c). On the other hand, ilmenites across veins display zonation, such that $Cr_2O_3$ in the ilmenite is much higher along the edges or margins of veins (Zhang 1998). The width of the high $Cr_2O_3$ zone is strongly dependent on the thickness of the vein, but is generally restricted to bands of approximately 1 mm for the wider veins ($> 5$ mm across), and of $< 0.5$ mm for the narrower veins ($< 5$ mm across). The wider veins have well-developed flat-bottomed minima and a very high $Cr_2O_3$ content at the extreme edge of the rim, whereas the narrow veins are sharp-bottomed with relatively low $Cr_2O_3$ contents at the extreme edge of the rim (Wyatt and Lawless 1984). Some wider veins have zones of high $Cr_2O_3$. Thus, the ilmenite veins are compositionally inhomogeneous and, in rare cases, chromium variation within ca. 2-cm veins can betray the whole range of the rock.

Ilmenite compositions in BD2394 and BD344 vary considerably between the different textural types (Tables 1, 2 and Fig. 4b–c). Small and tiny disseminated ilmenites contrast with the coarse grains, in that the former have higher $Cr_2O_3$ and lower $TiO_2$ contents, and usually contain trace amounts of $Nb_2O_5$. However, there are no significant differences in $Al_2O_3$ and MgO contents between these types. Furthermore, one ilmenite occurring as lamellae in rutile has a very distinctive composition (Table 2 and Fig. 4a, c). Its $Cr_2O_3$ and MgO contents are the lowest, and its FeO the highest amongst all the ilmenites in the polymict peridotites. $Al_2O_3$ content is the highest in all the ilmenites in BD2394.

### *Rutile*

Rutile occurs either as small discrete grains/veinlets, as rims to ilmenites, or as tiny grains intimately intergrown with ilmenite (Table 3). Rutile contains $Cr_2O_3$ and FeO in the ranges 0.70–5.02 and 0.10–0.66 wt% respectively, and up to 0.55 wt% $Al_2O_3$ and 0.18 wt% MgO. Of greater interest is the relatively high $Nb_2O_5$ content in some grains (up to 3.20 wt%). In a plot of $Nb_2O_5$ versus $Cr_2O_3$ (Fig. 5), three grains fall within the field of "vein and accessory rutile", and another one within the field of "rutile in association with LIMA and YIHA or Arm"

**Table 1** Ilmenite compositions (wt%) in the Bultfontein polymict xenoliths, South Africa: samples JJG1414, BD344, and BD2666. *Discrete*, *coarse*, and *small* Discrete, coarse, and small ilmenite grains respectively. *Vein* Ilmenite occurring as veinlet. Discrete, coarse, and vein ilmenite composition is an average of 2–7 analyses within a single grain. *Core* and *rim* Composition of core and rim in a vein-like grain. *nd* Not detected

| Sample | JJG1414 | | | | | | | | BD344 | | | | | | BD2666 | | | | | | | |
|---|---|---|---|---|---|---|---|---|---|---|---|---|---|---|---|---|---|---|---|---|---|---|
| Ilmenite | Vein1 | | Vein2 | | Discrete | | | | Coarse | | | | Small | | Vein | | | | | | | |
| | Core | Rim | Core | Rim | | | | | | | | | | | | | | | | | | |
| $SiO_2$ | 0.28 | 0.33 | 0.32 | 0.26 | 0.31 | 0.33 | 0.36 | 0.30 | 0.33 | 0.33 | 0.34 | 0.39 | 0.31 | 0.35 | 0.31 | 0.33 | 0.33 | 0.30 | 0.30 | 0.30 | 0.32 | 0.35 |
| $TiO_2$ | 57.17 | 56.87 | 56.68 | 56.43 | 57.43 | 56.97 | 56.72 | 56.89 | 56.94 | 56.93 | 55.72 | 56.32 | 55.87 | 54.84 | 56.88 | 56.67 | 56.19 | 57.12 | 56.78 | 56.14 | 56.41 | 56.33 |
| $Al_2O_3$ | 0.56 | 0.51 | 0.61 | 0.83 | 0.71 | 0.56 | 0.68 | 0.54 | 0.44 | 0.38 | 0.44 | 0.44 | 0.46 | 0.53 | 0.36 | 0.42 | 0.43 | 0.45 | 0.50 | 0.55 | 0.52 | 0.44 |
| $Cr_2O_3$ | 2.04 | 3.82 | 2.29 | 3.37 | 2.05 | 1.96 | 2.08 | 2.08 | 2.09 | 1.26 | 1.34 | 0.96 | 2.93 | 2.67 | 1.32 | 1.33 | 2.16 | 1.82 | 1.71 | 2.23 | 1.83 | 1.83 |
| FeO | 25.75 | 23.40 | 25.68 | 24.62 | 25.47 | 25.56 | 24.78 | 26.17 | 27.75 | 27.92 | 26.98 | 28.84 | 26.67 | 28.45 | 28.17 | 28.00 | 28.36 | 27.96 | 27.55 | 27.85 | 26.90 | 27.75 |
| MnO | 0.13 | 0.10 | 0.15 | 0.11 | 0.22 | 0.17 | 0.16 | 0.12 | 0.11 | 0.11 | 0.03 | 0.17 | 0.09 | 0.13 | 0.16 | 0.12 | 0.20 | 0.17 | 0.21 | 0.15 | 0.19 | 0.18 |
| MgO | 13.88 | 14.45 | 13.66 | 13.88 | 13.94 | 13.79 | 14.21 | 13.45 | 12.66 | 12.49 | 12.09 | 12.35 | 12.75 | 12.18 | 12.52 | 12.53 | 12.41 | 12.45 | 12.61 | 12.50 | 12.86 | 12.53 |
| CaO | 0.06 | 0.04 | 0.08 | 0.05 | 0.07 | 0.03 | 0.08 | 0.04 | 0.05 | 0.01 | 0.04 | 0.04 | 0.03 | 0.00 | 0.01 | 0.01 | 0.00 | 0.03 | 0.03 | 0.10 | 0.04 | 0.02 |
| $Nb_2O_5$ | nd | nd | nd | nd | nd | 0.07 | nd | 0.04 | nd | nd | nd | nd | nd | nd | 0.12 | 0.20 | 0.16 | nd | 0.20 | 0.18 | 0.10 | 0.18 |
| Total % | 99.87 | 99.52 | 99.47 | 99.55 | 100.20 | 99.44 | 99.07 | 99.63 | 100.37 | 99.43 | 96.98 | 99.51 | 99.11 | 99.15 | 99.85 | 99.61 | 100.24 | 100.30 | 99.89 | 100.00 | 99.17 | 99.61 |

**Table 2** Ilmenite compositions (wt%) in the Bultfontein polymict xenoliths, South Africa: samples BD2666 and BD2394. *Coarse*, *small*, *tiny* Coarse, small, tiny ilmenite grains respectively. *Vein*, *Lam.*, and *Diss*. Ilmenite occurring as veinlet, lamellae in rutile, and disseminated phase respectively. Coarse and vein ilmenite composition is an average of 2–7 analyses within a single grain. *nd* Not detected

| Sample | BD2666 | | | | BD2394 | | | | | | | | | | | | | | | | | |
|---|---|---|---|---|---|---|---|---|---|---|---|---|---|---|---|---|---|---|---|---|---|---|
| Ilmenite | Vein | | | | Coarse | | Vein | | Small | | | | | | | Tiny | | | | | Lam. | Diss. |
| | ILM1 | ILM2 | ILM3 | ILM4 | | | ILM1 | ILM2 | | | | | | | | [a] | | | | [b] | | |
| $SiO_2$ | 0.37 | 0.29 | 0.31 | 0.23 | 0.31 | 0.29 | 0.32 | 0.33 | 0.33 | 0.23 | 0.32 | 0.37 | 0.35 | 0.36 | 0.29 | 0.31 | 0.33 | 0.45 | 0.33 | 0.35 | 0.31 | 0.29 |
| $TiO_2$ | 56.56 | 56.62 | 56.70 | 57.24 | 55.83 | 55.76 | 55.29 | 56.01 | 57.14 | 57.05 | 56.32 | 56.86 | 56.50 | 56.52 | 56.60 | 54.10 | 56.70 | 54.13 | 56.15 | 55.47 | 55.33 | 56.61 |
| $Al_2O_3$ | 0.41 | 0.48 | 0.54 | 0.58 | 0.57 | 0.45 | 0.49 | 0.40 | 0.42 | 0.31 | 0.45 | 0.42 | 0.43 | 0.45 | 0.52 | 0.55 | 0.46 | 0.53 | 0.41 | 0.42 | 0.65 | 0.44 |
| $Cr_2O_3$ | 1.47 | 1.58 | 1.75 | 2.02 | 2.34 | 1.81 | 2.92 | 1.96 | 1.78 | 1.25 | 1.21 | 1.73 | 1.35 | 1.27 | 1.81 | 3.17 | 2.34 | 3.51 | 2.55 | 2.91 | 0.86 | 2.41 |
| FeO | 28.20 | 27.51 | 27.79 | 26.70 | 26.61 | 27.22 | 27.51 | 27.49 | 28.18 | 28.43 | 28.18 | 27.83 | 28.59 | 28.14 | 27.41 | 29.77 | 27.51 | 28.28 | 28.44 | 27.70 | 34.74 | 27.79 |
| MnO | 0.27 | 0.18 | 0.23 | 0.16 | 0.21 | 0.22 | 0.07 | 0.21 | 0.12 | 0.31 | 0.12 | 0.00 | 0.24 | 0.17 | 0.07 | 0.16 | 0.11 | 0.20 | 0.00 | 0.15 | 0.00 | 0.11 |
| MgO | 12.36 | 12.61 | 12.51 | 12.97 | 12.92 | 12.37 | 12.30 | 12.27 | 12.54 | 12.37 | 12.65 | 12.63 | 12.51 | 12.48 | 12.50 | 11.93 | 12.55 | 12.08 | 12.10 | 12.31 | 7.67 | 12.21 |
| CaO | 0.00 | 0.00 | 0.01 | 0.11 | 0.05 | 0.04 | 0.05 | 0.04 | 0.01 | 0.03 | 0.00 | 0.00 | 0.02 | 0.02 | 0.01 | 0.00 | 0.01 | 0.01 | 0.00 | 0.03 | 0.06 | 0.03 |
| $Nb_2O_5$ | 0.20 | 0.17 | 0.20 | 0.24 | 0.10 | nd | 0.14 | 0.25 | 0.12 | nd | nd | 0.20 | nd | 0.17 | 0.11 | nd | nd | 0.80 | 0.05 | nd | nd | 0.10 |
| Total % | 99.84 | 99.44 | 100.04 | 100.25 | 98.94 | 98.16 | 99.09 | 98.96 | 100.64 | 99.98 | 99.25 | 100.04 | 99.99 | 99.58 | 99.32 | 99.99 | 100.01 | 99.99 | 100.03 | 99.34 | 99.62 | 99.99 |

[a]Tiny ilmenite overgrown with sulphide phase
[b]Contains 0.4 wt% $V_2O_5$

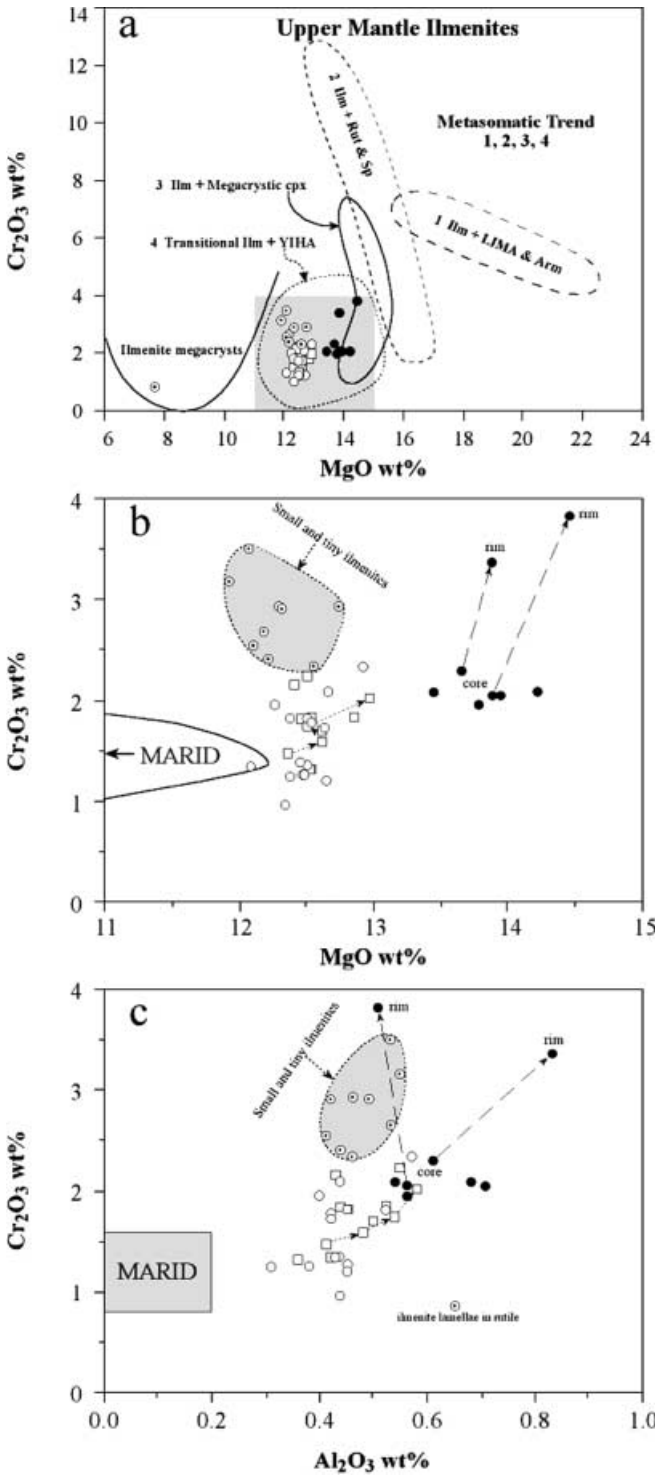


**Fig. 4a–c** Compositional variations in ilmenites from the polymict peridotites. **a** $Cr_2O_3$ versus MgO compared with those of upper mantle ilmenites from kimberlite megacrysts and kimberlite-borne mantle xenoliths. Metasomatic *trends 1*, *2*, and *3* Ilmenites in association with LIMA and Arm, with Rut and Sp, and with megacrystic Cpx respectively. *Trend 4* Ilmenites in association with YIHA (Haggerty 1991, 1994). All ilmenites from the polymict xenoliths fall within the trend-4 field. **b** Magnification of shaded field in **a**. *Solid circles* and *open squares* Ilmenites from JJG1414 and BD2666 respectively. *Open circles* Ilmenites from BD2394 and BD344 (*closed dots* ilmenite with smaller grain size). *Dotted arrow line* connecting four points indicates compositional variations in a veinlet of BD2666. *Dashed arrow line* connects two ilmenites in JJG1414 where the rim (*arrow end*) has much higher $Cr_2O_3$ content. **c** $Cr_2O_3$ versus $Al_2O_3$ (data for MARID field extracted from Dawson and Smith 1977). An ilmenite lamellae in rutile has the lowest MgO and $Cr_2O_3$

(Haggerty 1994). The chromium-rich, magnesium-poor and high-$Nb_2O_5$-bearing rutiles (termed as Nb-Cr-rutile; Haggerty 1983) are predominantly found in peridotites from the Kimberley pipes, South Africa (Jones et al. 1982; Wyatt and Lawless 1984; Tollo and Haggerty 1987). Similar high-$Cr_2O_3$ rutiles were reported in a suite of IRPS xenoliths from the Matsoku kimberlite in Lesotho (Harte et al. 1987). However, rutiles in IRPS rocks contain large amounts of $Ta_2O_5$ (up to 2.08 wt%) rather than $Nb_2O_5$ ( $\leq 0.3$ wt%). Rutiles documented by Jones et al. (1982) contain $ZrO_2$ (up to 1.0 wt%), BaO (0.23 wt%) and SrO (up to 0.65 wt%). Furthermore, rutile in MARID rocks (Dawson and Smith 1977) contains no niobium. Accommodation of chromium and niobium in rutile is ascribed to crystallographic shear in the structure (Haggerty 1994).

## Trace elements

Trace-element abundances in ilmenite and rutile (Fig. 6) are expressed as counts per second. All the ilmenites and rutiles analysed have LREE-enriched patterns whilst the element concentrations vary considerably between and within samples. Ilmenites from the polymict peridotite BD2666 show much higher trace-element abundances than those from JJG1414 (Fig. 6). In addition, all the trace-element CPS vary systematically along (BD2666) and across (JJG1414) ilmenite veins, and show highest trace-element abundance at the narrow end or in the rim (Fig. 6), particularly for the LREE, Sr, Nb, Cr, Al, and Ba. This is consistent with the results of the electron probe analysis for Cr and Al, and exhibits trace-element disequilibria in these ilmenites. Rutile coexisting in the ilmenite rim is extremely enriched in LREE, Nb, Zr, Ba, and Cr, but poor in Sr, Y, Ca, and Al, relative to the ilmenites.

## Oxygen isotopic ratios

Oxygen isotopes of ilmenites from the Bultfontein polymict peridotites, South Africa, are given in Table 4, and $\delta^{18}O‰$ values are plotted in Fig. 7. $\delta^{18}O$ values vary considerably in ilmenites of individual grains and rocks (Table 4 and Fig. 7). Coarser ilmenites from BD2394 and BD344 show a higher $\delta^{18}O$ than finer grains. An ilmenite overgrown with sulphide mineral from BD2394 has an extremely low $\delta^{18}O$ ($< 3‰$), whereas ilmenite from a vein in BD2666 has a range of $\delta^{18}O$ which ex-

**Table 3** Rutile compositions in the Bultfontein polymict peridotites. *nd* Not detected

| Sample | BD2394[b] | BD2394 | BD2394 | BD2394 | BD2394 | BD2394 | BD2394 | BD344 | JJG1414[c] | BD2666[c] | JJG513[c] |
|---|---|---|---|---|---|---|---|---|---|---|---|
| $SiO_2$ | 0.26 | 0.28 | 0.44 | 0.48 | 0.75 | 0.40 | 0.22 | 0.37 | nd | nd | nd |
| $TiO_2$ | 98.12 | 98.10 | 93.66 | 96.18 | 92.66 | 90.82 | 93.68 | 94.93 | 96.09 | 93.68 | 94.61 |
| $Al_2O_3$ | 0.55 | 0.21 | 0.09 | 0.05 | 0.09 | 0.15 | 0.12 | 0.10 | 0.06 | 0.12 | 0.03 |
| $Cr_2O_3$ | 0.70 | 0.90 | 4.94 | 2.79 | 2.88 | 5.02 | 2.53 | 3.56 | 3.09 | 2.53 | 3.21 |
| FeO[a] | 0.29 | 0.45 | 0.36 | 0.14 | 0.22 | 0.35 | 0.33 | 0.10 | 0.36 | 0.66 | 0.43 |
| MnO | 0.06 | 0.00 | 0.00 | 0.07 | 0.00 | 0.00 | 0.00 | 0.01 | nd | nd | nd |
| MgO | 0.02 | 0.07 | 0.05 | 0.08 | 0.05 | 0.17 | 0.18 | 0.03 | 0.12 | 0.18 | 0.11 |
| CaO | 0.03 | 0.02 | 0.05 | 0.00 | 0.00 | 0.02 | 0.02 | 0.05 | 0.01 | 0.02 | 0.02 |
| $Nb_2O_5$ | nd | nd | nd | nd | 3.41 | 3.20 | 2.80 | nd | nd | 2.81 | nd |
| Total % | 100.03 | 100.03 | 99.59 | 99.79 | 100.06 | 100.13 | 99.88 | 99.15 | 99.73 | 100.00 | 98.41 |

[a]Total Fe expressed as divalent FeO
[b]Rutile containing ilmenite lamellae
[c]Data extracted from Wyatt and Lawless (1984)

tends to higher oxygen isotope ratios ($> 5‰$). The core in the vein ilmenite from JJG1414 is richer in $^{18}O$ than the rim, with a maximum fractionation of $\sim 0.8‰$ between the core and the rim, corresponding to the variation in $Cr_2O_3$ (Fig. 7). An ilmenite vein from BD2666 shows a systematic variation in $\delta^{18}O$ along the length of the vein. This is consistent with the elemental variation, such as for $Cr_2O_3$ (Fig. 7), LREE, and LILE (Fig. 6). More than $1.4‰$ $\delta^{18}O$ fractionation over a distance of ca. 2 cm may indicate oxygen isotope disequilibrium. Analyses from the centre of a wider vein show a similar $\delta^{18}O$ signature as coarse ilmenite from BD2394 and BD344, the core of vein ilmenite from JJG1414, and ilmenite from the Amalia garnet peridotite, South Africa (Fig. 7). It is obvious that the oxygen isotopic ratios in ilmenites vary with the texture and elemental compositions (Fig. 7). In general terms, fine-grained high-chromium ilmenite has a lighter $\delta^{18}O$, and coarse-grained low-chromium ilmenite has a heavier $\delta^{18}O$. Thus, the process which produced the oxygen isotope depletion is the process which caused the chromium and trace-element enrichment.

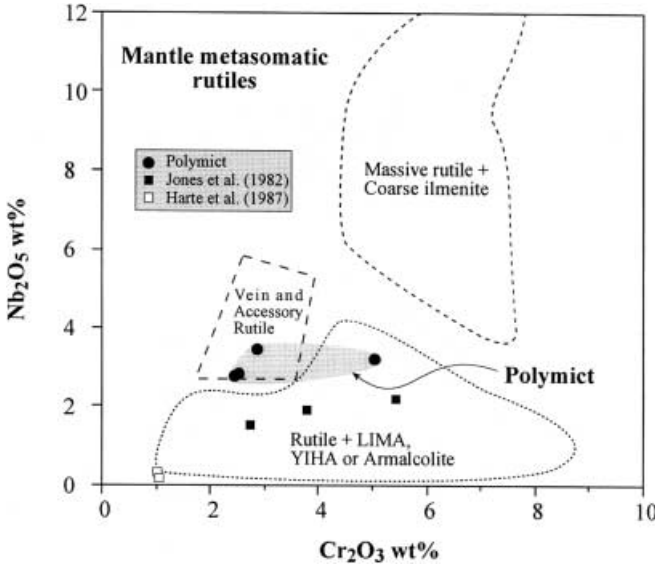


**Fig. 5** $Cr_2O_3$ versus $Nb_2O_5$ in rutiles from the polymict peridotites, South Africa, and other kimberlite-borne mantle xenoliths (Jones et al. 1982; Harte et al. 1987). The fields of massive rutile, vein and accessory rutile, and rutile in association with LIMA and YIHA or armalcolite are after Haggerty (1994)

## Discussion

### Petrogenesis, melt infiltration and disequilibrium

The oxide mineral paragenesis (i.e. ilmenite + rutile ± sulphide association) in the polymict peridotites from the Bultfontein kimberlites is similar to those in other kimberlite-borne metasomatic xenoliths (e.g. Jones et al. 1982), and in the IRPS suite from the Matsoku kimberlites (Harte et al. 1987). This paragenesis is different from those derived from the MARID suite (Dawson and Smith 1977; Waters 1987), in which ilmenite is very low in MgO and $Al_2O_3$ (Fig. 4b–c). Detailed textural, elemental and oxygen isotopic studies strongly suggest a magmatic and/or metasomatic origin for the oxides from the polymict xenoliths (Fig. 4a). The ilmenite texture and its relationship with silicate minerals indicate the presence of a melt transfer process, i.e. a magmatic process. These ilmenites, in particular the coarse ones and those occurring as veins, appeared to have crystallised directly from the trapped Fe-Ti-rich melt. However, all the ilmenites, including the coarse ones and those occurring as veins, have transitional chemical characteristics between kimberlite-borne megacrysts and the metasomatic trend, and they plot with YIHA (Fig. 4a). Thus, the magmatic process which formed the coarse and vein-like ilmenites is different from the magmatic process of kimberlites which crystallised the ilmenite megacrysts. Similarly, rutiles in these polymict xenoliths have chemical compositions which fall within those for kimberlitic accessories and rutiles associated with LIMA + YIHA (Fig. 5), typical of

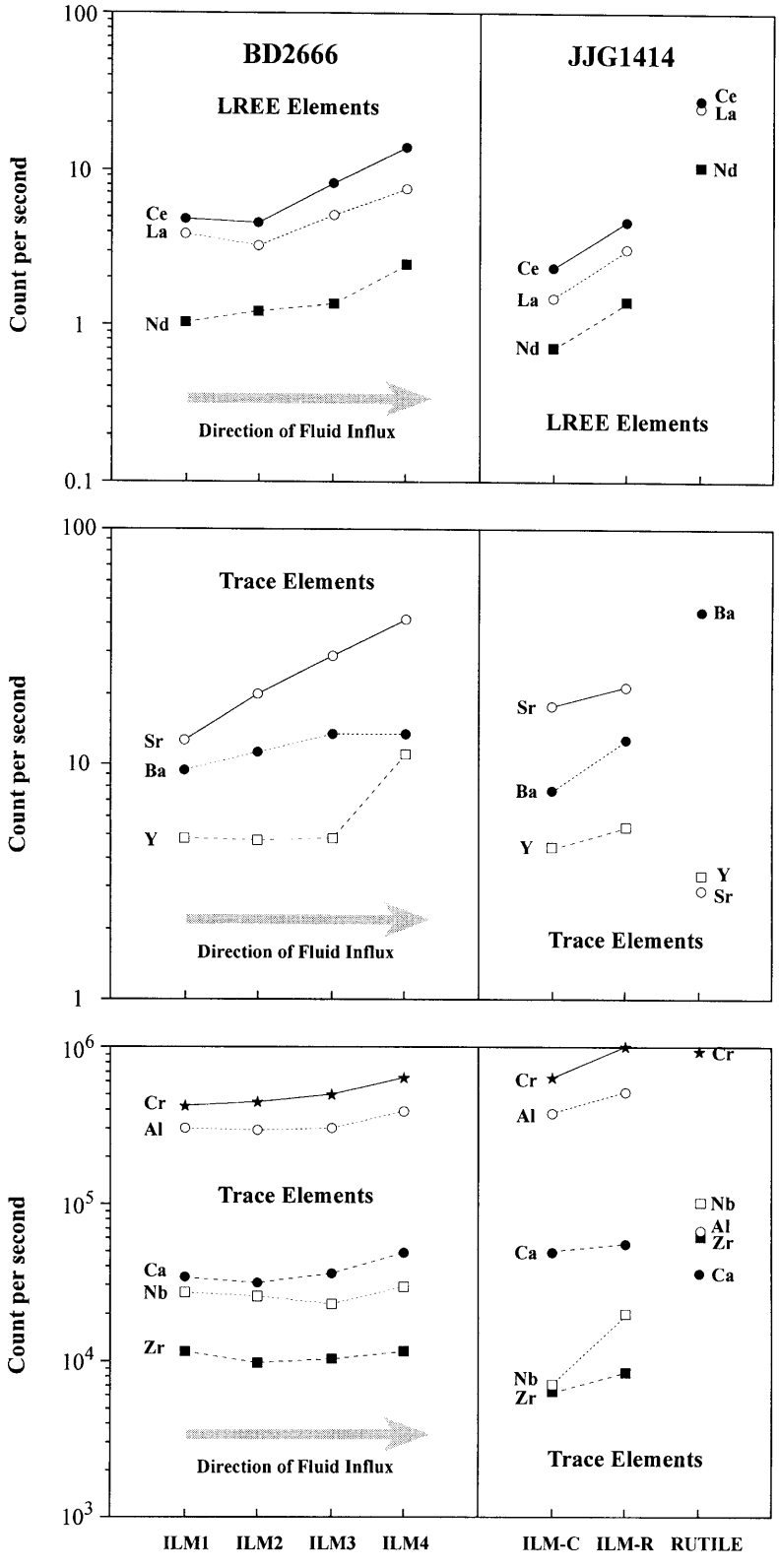


**Fig. 6** Qualitatively elemental variations of ilmenites and rutile from the Bultfontein polymict peridotites, South Africa. *ILM1–ILM4* Analyses in sequence along an ilmenite vein, with the corresponding photograph shown in Fig. 2b. *ILM-C* and *ILM-R* Core and rim composition across an ilmenite vein in JJG1414 (Fig. 1c). *RUTILE* Small irregular rutile coexisting with ilmenite (element abundance expressed as counts per second)

highly metasomatic minerals (Haggerty et al. 1983, 1986; Erlank et al. 1987; Haggerty et al. 1989). This indicates that a simple magmatic process apparently cannot account for the observed chemical features of these oxides, especially the tiny and disseminated ilmenites and rutiles. Also, the possibility of isochemical decomposition proposed by Wyatt (1979) for trace ilmenite-rutile appears not to be the case, since the initial mineral armalcolite is absent and the large amount of discrete ilmenite is difficult to account for by isochemical de-

**Table 4** Oxygen isotopic ratios in ilmenite from the Bultfontein polymict peridotites, South Africa. $Cr_2O_3$ content is electron probe data (wt%)

| Sample | JJG1414 | | | | | BD344 | | BD2666 | | | | | BD2394 | | | |
|---|---|---|---|---|---|---|---|---|---|---|---|---|---|---|---|---|
| Ilmenite | Vein1 | | Vein2 | | Discrete | Coarse | Small | Vein | | | | | Coarse | | Vein ILM2 | Small | Tiny[a] |
| | Core | Rim | Core | Rim | | | | | ILM1 | ILM2 | ILM3 | ILM4 | | | | | |
| $\delta^{18}O$ (‰) | 4.63 | 3.78 | 4.25 | 4.00 | 4.50 | 3.92 | 3.85 | 4.05 | 3.86 | 5.17 | 4.84 | 4.09 | 3.70 | 4.23 | 3.94 | 4.07 | 3.67 | 2.90 |
| Yield (%) | 96.9 | 101.0 | 97.6 | 101.7 | 98.2 | 100.6 | 98.8 | 97.5 | 98.7 | 97.0 | 97.3 | 100.3 | 102.3 | 97.3 | 97.1 | 98.5 | 98.9 | 97.4 |
| $Cr_2O_3$ | 2.04 | 3.82 | 2.29 | 3.37 | 2.08 | 2.09 | 2.67 | 1.83 | 2.16 | 1.47 | 1.58 | 1.75 | 2.02 | 1.81 | 2.34 | 1.96 | 1.73 | 3.17 |

[a]Tiny ilmenite overgrown with sulphide phase

composition (this study; Tollo and Haggerty 1987). Therefore, a metasomatic process, i.e. Fe-Ti-rich melt infiltration must be invoked in the origin of these oxides, consistent with the petrologic observations and elemental chemistry of coexisting silicate minerals (Zhang 1998). Melt infiltration resulted in a complexity of silicate minerals (Zhang 1998), and a variety of oxide minerals.

LREE and LILE enrichments in these oxide minerals (Fig. 6), and large chemical and oxygen isotopic variations in different texture ilmenites (Figs. 6, 7) generally support the assumption that the rocks were subjected to multiple stages of melt transfer and/or infiltration. The coarser, smaller, and disseminated ilmenites seem not to be the products of the same stages. The high $Cr_2O_3$ content and oxygen isotope depletion in the small and tiny disseminated ilmenite may represent the very late stages of melt infiltration and precipitation at very low temperatures. The absence of armalcolite, LIMA and YIHA in the polymict samples is probably in part due to the diversity of melt composition and precipitation at depth. These minerals coexist with richterite or spinel, and are formed via water-bearing metasomatism under oxidised conditions at 75–100 km. Thus, we conclude that the Fe-Ti-Cr-rich melt infiltration led to the systematic change in major elements (Fig. 4), trace elements (Fig. 6), and oxygen isotopes (Fig. 7) along and across ilmenite veins. In other words, the oxide minerals in these polymict rocks retain the extreme intergrain and intragrain chemical and oxygen isotopic disequilibrium, similar to the silicate minerals (Zhang 1998; Zhang et al. 2000). Textural, elemental and $\delta^{18}O$ zonation in ilmenites and $>1.4‰$ fractionation in an ilmenite vein over a distance of ca. 2 cm may indicate that melt infiltration is recent. Melt infiltration also led to the coeval crystallisation of ilmenite needles (Fig. 2c) in neoblastic olivine crystal. After melt infiltration, diffusion metasomatism under the subsolidus occurred between the oxides and the adjacent silicate minerals, as evidenced by the lower oxygen isotopic ratios in smaller ilmenite grains and in the rims of ilmenite veins. However, this subsolidus diffusion between mineral grains was far from complete, due to the presence of well-preserved chemical and oxygen isotopic disequilibrium in the oxides. The elemental diffusion may also have been terminated by mantle deformation which led to mineral recrystallization, as shown by the existence of the common triple junctions in the centre of the coarse or vein-like ilmenites.

## Possible origin of Fe-Ti-Cr-rich melt in the mantle

The vein-like aspect of the ilmenite in JJG1414 and BD2666 led Wyatt and Lawless (1984) to suggest an "intrusive" origin from a "hydrous-$TiO_2$-$K_2O$-rich liquid". These authors suggested the high-Cr ilmenite rims are derived from earlier crystallisation of the melt at

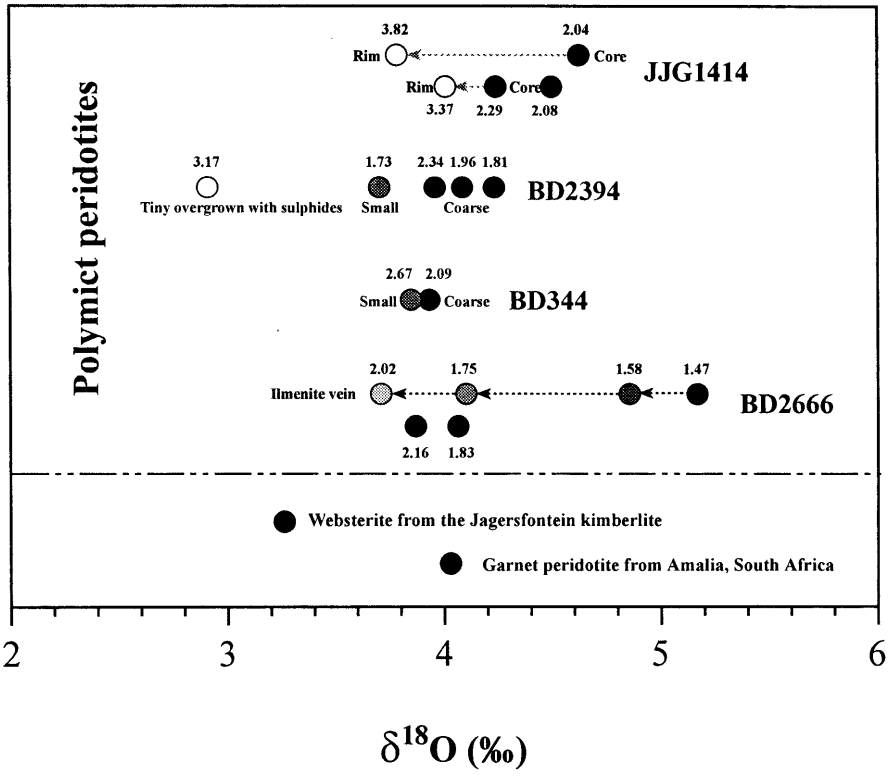


**Fig. 7** Oxygen isotopic compositions of ilmenites from the Bultfontein polymict xenoliths, with the $Cr_2O_3$ content (wt%) given for comparison. Oxygen isotopic values of ilmenites from a Jagersfontein websterite and an Amalia garnet peridotite, South Africa, are after Lowry (personal communication). The *symbol* is about the size of the analytical uncertainty

high temperature. However, the fact that the high-Cr ilmenite rims and rutile only occur along the margins of ilmenite veins possibly indicates that they are the products of the melt at late stage. Even though the dispute on the formation of ilmenite rims still exists, the large influx of Fe-Ti-Cr-rich, possibly K-rich melt into the peridotite precursor can account for all the chemical and oxygen isotopic characteristics observed in the oxide minerals as well as silicate minerals of these unique polymict xenoliths (Zhang 1998). The different textures in ilmenites may crystallise at different stages of the melt, with the tiny disseminated ilmenites being formed at the latest stage. Thus, melt infiltration just prior to the kimberlite entrainment may be one of the major causes which led to the commonly observed textural, elemental and oxygen isotopic disequilibria in the polymict minerals. This suggests that the melt responsible for the ilmenite crystallisation is compositionally similar to the melt which produced the IRPS suite xenoliths from Matsoku (Harte et al. 1987). The existence of highly titaniferous melts in the mantle is also supported by a xenolith from the Weltevreden Mine, which is composed of quench ilmenite and pyroxene (Rawlison and Dawson 1979).

The Fe-Ti-Cr-rich melt may originate at depth but can not be formed directly by the partial melting of normal mantle peridotite because there would be insufficient Fe and Ti. A reasonable explanation is that the melt was at high temperature and pressure segregation, in terms of high MgO content in ilmenites. It was formed by melt immiscibility from originally homogeneous silicate melt (protokimberlitic or protolamproitic), similar to the formation of Fe-Ti-rich melt found in some ultrabasic complexes such as Bushveld (Scoon and Mitchell 1994, and references therein). The high-Fe-Ti-oxide melts, immiscibly separated from fractionating alkali basalt at magmatic temperatures, have been observed in the Western Carpathians, Slovakia (Hurai et al. 1998). A close genetic relationship between Fe-Ti-oxide-rich xenoliths and mantle-derived basaltic magma is also documented by mineral $^{18}O$ values. Kimberlites are well known to be enriched in ilmenites (Dawson 1980; Mitchell 1986), and the silicate melt which generated the kimberlite must be rich in Fe and Ti. Ilmenite phenocrysts from kimberlites (Haggerty 1975) and basalts (Anderson and Wright 1972) are also characterised by the compositional zonation with higher MgO contents at the margins, similarly to ilmenites from the polymict peridotites. The Mg zoning in ilmenite is probably merely a reflection of Mg-Fe exchange upon cooling. Fe and Mg diffuse faster in ilmenite than in olivine, with the result that the ilmenite-olivine thermometer is not applicable to plutonic assemblages (Andersen et al. 1991). When this high-temperature and high-pressure melt, initiated in the asthenosphere, infiltrated into the cold lithosphere, it may have produced highly Fe-Ti-enriched segregation due to melt immiscibility under certain circumstances. Thus, the Ti-Fe-Cr-rich melt derivatives should be highly localised, and logically have high ilmenite normative. Infiltration of this melt through mantle peridotites would lead to the enrichment of Fe-Ti-rich oxides in these peridotites.

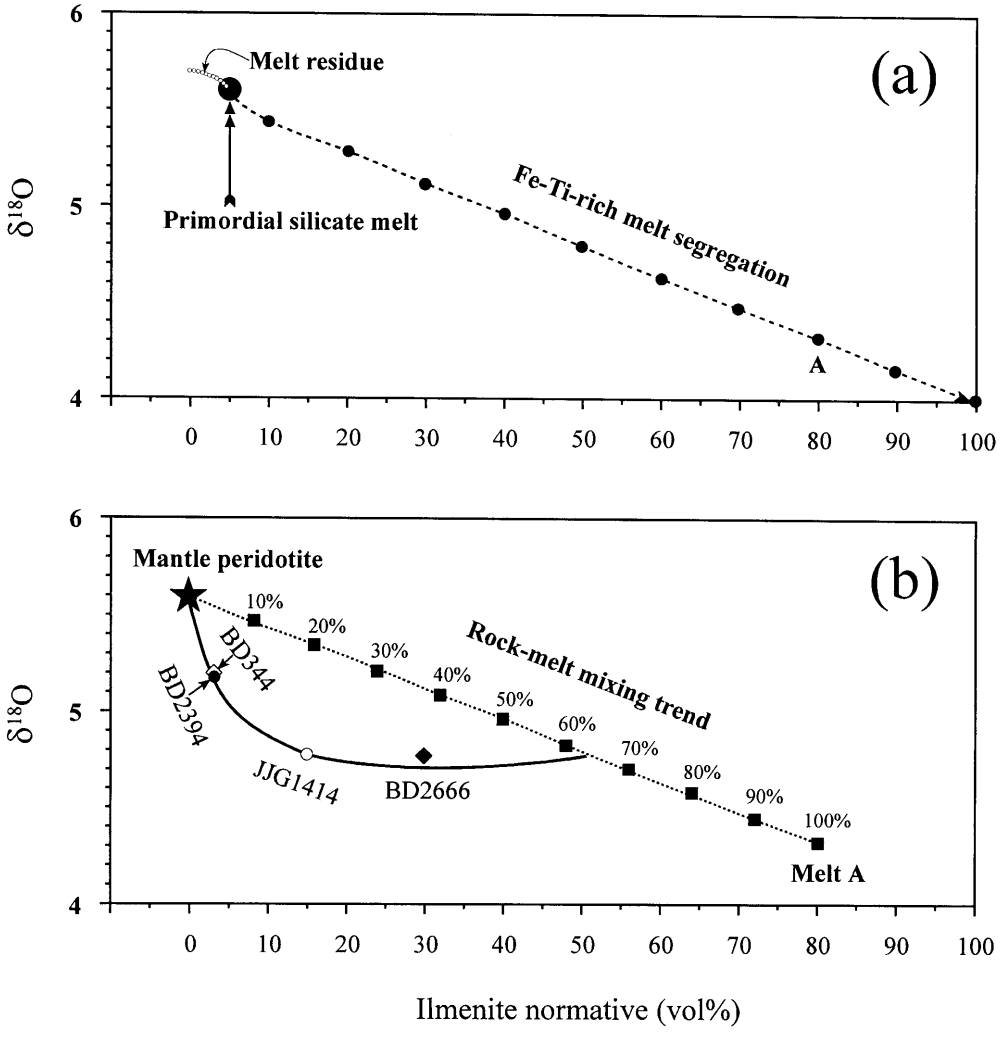


**Fig. 8** **a** Illustrates the formation of low-$\delta^{18}O$, high-Fe-Ti-oxide melt segregation by magma immiscibility from a titaniferous silicate melt which has a $\delta^{18}O$ similar to MORB (5.6‰). *Curved line* Compositional variation trend of melt residue. **b** Illustrates the reaction trend between mantle peridotite ($\delta^{18}O = 5.6$‰) and newly segregated *melt A* (80% ilmenite normative) in close system. The bulk oxygen isotopic ratios of the polymict peridotites were calculated from the mineral modes and the measured $\delta^{18}O$ values of individual mineral phases. Note that all the polymict xenoliths plot below the simple mixing line

## Implications for low bulk-rock oxygen isotopic ratios

As mentioned above, ilmenites are lower in oxygen isotopes (~3.7–4.9‰) than the silicate minerals (generally in the range of ~4.6–6.2‰) in the polymict peridotites (Zhang et al. 2000). This, in turn, is lighter in $\delta^{18}O$ than the corresponding silicate minerals from diamond-, garnet- and spinel-facies mantle xenoliths (Lowry et al. 1994; Mattey et al. 1994a, 1994b). Oxygen isotope fractionation between minerals and/or melts mainly depends on the structure of the mineral or melt and the temperature (Kyser 1986, 1990; Zheng 1993a, 1993b; Mattey et al. 1994a). Overall, the simpler the structure and the lower the temperature, the lighter the oxygen isotope ratio (olivine < pyroxene < amphibole < plagioclase < quartz in $\delta^{18}O$). Thus, it seems possible that the lighter oxygen isotope is preferentially fractionated into the Fe-Ti-oxide-rich melt portion, leading to the formation of localised low oxygen-isotope melt and relatively high oxygen-isotope residue of silicate melt. The infiltration of low $\delta^{18}O$, transient melt segregation along mantle faults/fractures finally produced the oxygen isotope characteristics of the polymict xenoliths.

Figure 8 illustrates the formation of low-$\delta^{18}O$, high-Fe-Ti-oxide melt segregation by magma immiscibility from a titaniferous silicate melt, and of low bulk $\delta^{18}O$ rocks by the reaction between normal mantle peridotite and the newly segregated melt. Laser fluorination analyses for minerals from a large variety of kimberlite- and basalt-borne mantle xenoliths (i.e. diamond-spinel phases, low-T granular to high-T sheared, dry-wet peridotites) show that the dominant mantle portions are homogenous in oxygen isotope compositions (Mattey et al. 1994a, 1994b). The bulk oxygen isotopic ratio in mantle rocks, calculated from $\delta^{18}O$ values and modes of the constituent minerals (OL + OPX + CPX + GT or SP), converges on $5.6 \pm 0.2$‰. Assuming that the primordial titaniferous melt (e.g. protokimberlite) was in equilibrium with, or was buffered by, mantle wall rock, the melt should have the same oxygen isotopic ratio as the peridotite. Thus, we take 5.6‰ for a good approximation of the oxygen isotopic ratio in the melt. This approximation is supported by the oxygen isotopic data from the fresh Cretaceous Mid-Ocean Range Basalts (MORB), which gave an astonishing uniformity in $\delta^{18}O$ ($+5.6 \pm 0.3$‰; Muehlenbachs and Clayton 1972;

Gregory and Taylor 1981). The oxygen isotopic ratio in ilmenite is deduced from the $\delta^{18}O$ modal value of ilmenites from the polymict xenoliths (4.0‰). Thus, the ilmenite normative-rich melt segregated from an original homogenous melt has a significantly low oxygen isotopic ratio (Fig. 8a). Consequently, the residue should have a subtle increase in $\delta^{18}O$, with the maximum at the time when no ilmenite normative is present in the melt. Similarly, the addition of the Fe-Ti-oxide-rich melt into the normal mantle peridotites can significantly lower the oxygen isotopes in the resultant rocks (Fig. 8b). However, the simple mixing (i.e. in a closed system) of mantle peridotite and melt can not account for the relative low ilmenites in the polymict xenoliths, whereas it is in good agreement with the low bulk oxygen isotopes in these rocks. This may indicate that more complicated processes have been involved in the generation of these polymict rocks, rather than just a simple rock-melt interaction, consistent with the complex petrological, mineralogical and geochemical appearance.

## Conclusions

Detailed investigations of the petrology, mineralogy and geochemistry of the oxide minerals in these polymict xenoliths lead to the following conclusions.

1. Oxide mineral assemblages in these polymict peridotites are petrologically of ilmenite dominance. These contrast markedly with dominant kimberlite-borne mantle xenoliths from the Kaapvaal craton in which the spinel minerals dominate. However, the mineral assemblages (ilmenite + rutile + sulphide + phlogopite) are very similar to the IRSP suite and some metasomatised xenoliths from southern Africa.
2. Oxide minerals have a texture as complex as those of silicate minerals, indicating a complex origin.
3. Ilmenites are richer in Cr, Mg, and Al than those in other metasomatic assemblages at Bultfontein. Marked chemical variations along and across the veins indicate the complexity of the "late" fluid process. The textural and major elemental zonations within the ilmenites are also demonstrated by the trace elemental and oxygen isotopic zonation. All these chemical and oxygen isotopic variations may be associated with melt transfer processes.
4. Isotope modelling shows that the influxes of Fe-Ti-Cr-rich melt into normal mantle can produce peridotites with low oxygen isotopes as observed in the polymict peridotites, but the rock-melt reaction may be more complicated than just a simple mixing.

**Acknowledgements** The Overseas Research Student Scheme (UK) and K.C. Wong Education Foundation (Hong Kong) are thanked for joint financial support in a studentship at the Royal Holloway University of London. This paper is part of a doctoral thesis (HZ). Funds from the Chinese Academy of Sciences (KZCX1–07) and the Ministry of Personnel of China are also gratefully acknowledged. Special thanks are given to B. Ronald Frost and Stephen E. Haggerty for thorough and constructive reviews, which resulted in great improvement of the paper.

## References

Andersen DJ, Bishop FC, Lindsley DH (1991) Internally consistent solution models for Fe-Mg-Mn-Ti oxides: Fe-Mg-Ti oxides and olivine. Am Mineral 76:427–444

Anderson AT, Wright TL (1972) Phenocrysts and glass inclusions and their bearing on oxidation and mixing of basaltic magmas, Kilauea volcano, Hawaii. Am Mineral 57:188–216

Dawson JB (1980) Kimberlites and their xenoliths. Springer, Berlin Heidelberg New York

Dawson JB, Smith JV (1977) The MARID (mica-amphibole-rutile-ilmenite-diopside) suite of xenoliths in kimberlite. Geochim Cosmochim Acta 41:309–323

Erlank AJ, Waters FG, Hawkesworth CJ, Haggerty SE, Allsopp HL, Rickard RS, Menzies MA (1987) Evidence for mantle metasomatism in peridotite nodules from Kimberley pipes, South Africa. In: Menzies MA, Hawkesworth CJ (eds) Mantle metasomatism. Academic Press, New York, pp 221–311

Gregory RT, Taylor HP (1981) An oxygen isotope profile in a section of Cretaceous oceanic crust, Samail ophiolite, Oman: evidence for $\delta^{18}O$-buffering of the oceans by deep (> 5 km) seawater-hydrothermal circulation at mid-ocean ridges. J Geophys Res 86:2737–2755

Gurney JJ, Jakob WRO, Dawson JB (1979) Megacrysts from the Monastery kimberlite pipe, South Africa. In: Boyd FR, Meyer HOA (eds) The mantle samples: inclusions in kimberlites and other volcanics. Proc 2nd Int Kimberlites Conf 2, October 1977, Santa Fe, pp 227–243

Haggerty SE (1975) The chemistry and genesis of oxide minerals in kimberlite. Phys Chem Earth 9:295–307

Haggerty SE (1983) The mineral chemistry of new titanates from a Jagersfontein kimberlite, South Africa: implication for metasomatism in the upper mantle. Geochim Cosmochim Acta 47:1833–1854

Haggerty SE (1991) Oxide mineralogy of the upper mantle. In: Lindsley DH (ed) Oxide minerals: petrologic and magnetic significance. Miner Soc Am Rev Mineral 25: 355–416

Haggerty SE (1994) Upper mantle mineralogy. J Geodyn 20:331–364

Haggerty SE, Hardie RB, McMahon RM (1979) The mineral chemistry of ilmenite nodule associations from the Monastery diatreme. In: Boyd FR, Meyer HOA (eds) The mantle sample: Inclusions in kimberlites and other volcanics. Proc 2nd Int Kimberlites Conf 2, October 1977, Santa Fe, pp 249–256

Haggerty SE, Smyth JR, Erlank AJ, Richard RS, Danchin RV (1983) Lindsleyite (Ba) and mathiasite (K): Two new chromium titanates in the crichtonite series from the upper mantle. Am Mineral 68:494–505

Haggerty SE, Erlank AJ, Grey IE (1986) Metasomatic mineral titanate complexing in the upper mantle. Nature 319:761–763

Haggerty SE, Crey IE, Madsen IC, Criddle AJ, Stanley CJ, Erlank AJ (1989) Hawthorneite, $Ba(Ti_3Cr_4Fe_4Mg)O_{19}$: a new metasomatic magnetoplumbite-type mineral from the upper mantle. Am Mineral 74:668–675

Harte H, Winterburn PA, Gurney JJ (1987) Metasomatic and enrichment phenomena in garnet peridotite facies mantle xenoliths from the Matsoku kimberlite pipe, Lesotho. In: Menzies MA, Hawkesworth CJ (eds) Mantle metasomatism. Academic Press, New York, pp 145–220

Hurai V, Simon K, Wiechert U, Hoefs J, Konecny P, Huraiova M, Ironon JP, Lipka J (1998) Immiscible separation of metalliferous Fe/Ti-oxide melts from fractionating alkali basalt: P-T-$fO_2$ conditions and two-liquid elemental partitioning. Contrib Mineral Petrol 133:12–29

Jones AP, Smith JV, Dawson JB (1982) Mantle metasomatism in 14 veined peridotites from Bultfontein mine, South Africa. J Geol 90:435–453

Kyser TK (1986) Stable isotope variations in the mantle. In: Vally JW, Taylor J, O'Neil JR (eds) Stable isotopes in high temperature geological processes. Miner Soc Am Rev Mineral 16:141–164

Kyser TK (1990) Stable isotopes in the continental lithospheric mantle. In: Menzies MA (ed) Continental mantle. Clarendon, Oxford, pp 127–156

Lawless PJ, Gurney JJ, Dawson JB (1979) Polymict peridotites from the Bultfontein and De Beers mines, Kimberley, South Africa. In: Boyd FR, Meyer HOA (eds) The mantle sample: inclusions in kimberlites and other volcanics. Proc 2nd Int Kimberlites Conf 2, October 1977, Santa Fe, pp 145–155

Lowry D, Mattey DP, Macpherson CG, Harris JW (1994) Evidence for stable isotope and chemical disequilibrium associated with diamond formation in the mantle. Mineral Mag 58A:535–536

Mattey D, Macpherson C (1993) High-precision oxygen isotope microanalysis of ferromagnesian minerals by laser-fluorination. Chem Geol 105:305–318

Mattey DP, Lowry D, Macpherson CG (1994a) Oxygen isotope composition of mantle peridotite. Earth Planet Sci Lett 128:231–241

Mattey DP, Lowry D, Macpherson CG, Chazot G (1994b) Oxygen isotope composition of mantle minerals by laser fluorination analysis: homogeneity in peridotites, heterogeneity in eclogites. Mineral Mag 58A:573–574

Meyer HOA, Tsai HM, Gurney JJ (1979) A unique enstatite megacryst with coexisting Cr-poor and Cr-rich garnet, Weltevreden floors, South Africa. In: Boyd FR, Meyer HOA (eds) The mantle sample: inclusions in kimberlites and other volcanics. Proc 2nd Int Kimberlites Conf 2, October 1977, Santa Fe, pp 279–291

Mitchell RH (1986) Kimberlites: mineralogy, geochemistry, and petrology. Plenum, London

Muehlenbachs K, Clayton RN (1972) Oxygen isotope studies of fresh and weathered submarine basalts. Can J Earth Sci 8:172–184

Pasteris JD, Boyd FR, Nixon PH (1979) The ilmenite association at the Frank Smith, R.S.A. In: Boyd FR, Meyer HOA (eds) The mantle sample: inclusions in kimberlites and other volcanics. Proc 2nd Int Kimberlites Conf 2, October 1977, Santa Fe, pp 265–278

Rawlinson PJ, Dawson JB (1979) A quench pyroxene-ilmenite xenolith from kimberlite: Implications for pyroxene-ilmenite intergrowths. In: Boyd FR, Meyer HOA (eds) The mantle sample: inclusions in kimberlites and other volcanics. Proc 2nd Int Kimberlites Conf 2, October 1977, Santa Fe, pp 292–299

Scoon RN, Mitchell AA (1994) Discordant iron-rich ultramafic pegmatites in the Bushveld complex and their relationship to iron-rich intercumulus and residual liquids. J Petrol 35:881–917

Tollo RP, Haggerty SE (1987) Nb-Cr-rutile in the Orapa kimberlite, Botswana. Can Mineral 25:251–264

Waters FG (1987) A suggested origin of MARID xenoliths in kimberlites by high-pressure crystallization of an ultrapotassic rock such as lamproite. Contrib Mineral Petrol 95:523–533

Wyatt B (1979) Kimberlitic chromian picroilmenites with intergrowths of titanian chromite and rutile. In: Boyd FR, Meyer HOA (eds) The mantle sample: inclusions in kimberlites and other volcanics. Proc 2nd Int Kimberlites Conf 2, October 1977, Santa Fe, pp 257–264

Wyatt BA, Lawless PJ (1984) Ilmenite in polymict xenoliths from the Bultfontein and De Beers mines, South Africa. In: Kornprobst J (ed) Kimberlites II: the mantle and crust-mantle relationships. Proc 3rd Int Kimberlites Conf 2, September 1982, Clermont Ferrand, pp 43–56

Zhang H-F (1998) Petrology and geochemistry of on- and off-craton mantle rocks: eastern China and southern Africa. PhD Thesis, Royal Holloway University of London

Zhang H-F, Mattey DP, Grassineau N, Lowry D, Brownless M, Gurney JJ, Menzies MA (2000) Recent fluid processes in the Kaapvaal craton, South Africa: coupled oxygen isotope and trace element disequilibrium in polymict peridotites. Earth Planet Sci Lett 57:57–72

Zheng Y-F (1993a) Calculation of oxygen isotope fractionation in hydroxyl-bearing silicate minerals. Earth Planet Sci Lett 120:247–263

Zheng Y-F (1993b) Calculation of oxygen isotope fractionation in anhydrous silicate minerals. Geochim Cosmochim Acta 57:1079–1091